

Multiperiodic Galactic field RR Lyrae stars in the ASAS catalog

D. M. Szczygieł^{1*} and D. C. Fabrycky^{2†}

¹*Warsaw University Observatory, Al. Ujazdowskie 4, 00-478 Warsaw, Poland*

²*Princeton University Observatory, Peyton Hall, Princeton, NJ 08544, USA*

Accepted –. Received –; in original form –

ABSTRACT

The All Sky Automated Survey (ASAS) monitors bright stars ($8 \text{ mag} < V < 14 \text{ mag}$) south of declination $+28^\circ$. The ASAS Catalogue of Variable Stars (ACVS) presently contains 50,099 objects; among them are 2212 objects classified as RR Lyrae pulsating variables. We use ASAS photometric V band data to search for multiperiodicity in those stars. We find that 73 of 1435 RRab stars and 49 of 756 RRC stars exhibit the Blazhko effect. We observe a deficiency of RRab Blazhko variables with main pulsation periods greater than 0.65 days. The Blazhko periods of RRC stars exhibit a strongly bimodal distribution. During our study we discovered the Blazhko effect with multiple periods in object ASAS 050747-3351.9 = SU Col. Blazhko periods of 89.3 d and 65.8 d and a candidate of 29.5 d were identified with periodogram peaks near the first three harmonics of the main pulsation. These observations may inspire new models of the Blazhko effect, which has eluded a consistent theory since its discovery about one hundred years ago. Long term lightcurve changes were found in 29 stars. We also found 19 Galactic double mode pulsators (RRd), of which 4 are new discoveries, raising the number of ASAS discoveries of such objects to 16, out of 27 known in the field of our Galaxy.

Key words: stars: pulsating – stars: variables: RR Lyrae

1 INTRODUCTION

The discovery of RR Lyrae stars in star clusters (Bailey 1902) led to some of the first studies of radial pulsations in stars (Shapley 1914, Eddington 1917) as well as distance determinations based on stellar variability (Shapley 1918). Recent surveys have searched for substructure in the Milky Way, attributed to the incorporation of satellite galaxies, via overdensities of RR Lyrae stars (Duffau et al. 2006). Their pulsation means they lie in the instability strip of the Hertzsprung-Russell diagram, the extent (and metallicity dependence) of which may be evaluated based on a statistical sample of such stars. Finally, RR Lyrae stars are found to pulsate not just with a single period, but in multiple radial and non-radial modes of different period, which gives constraints both to pulsation theory and to internal structure calculations. The current study presents the photometric signal of these multiperiodic phenomena in a large sample of RR Lyrae stars.

In Section 2 we shortly describe ASAS experiment and

its database, as well as the RR Lyrae sample derived from the ASAS Catalogue of Variable Stars. Sections 3 and 4 contain the method and results of multiperiodicity search, together with the discussion. Finally in Section 5 we summarize the results.

2 ASAS DATA

2.1 The All Sky Automated Survey

The ASAS project is located in Las Campanas Observatory in Chile and currently consists of two small, wide-field telescopes (200/2.8) with $2K \times 2K$ CCD cameras with 15μ pixel size from Apogee, observing in standard V and I filters. The main goal of the ASAS project is to monitor the whole available bright ($8 \text{ mag} < V < 14 \text{ mag}$) sky and search for variability. It has been observing south of declination $+28^\circ$ (almost 75% of the whole sky) since 2000, and a smaller part since 1997, covering the available sky every 1-3 nights. The project is ongoing, but has already yielded a few hundred photometric measurements per star.

Analysis of the V band data taken over the last 6 years resulted in the ASAS Catalog of Variable Stars

* e-mail: dszczyg@astrouw.edu.pl

† e-mail: dfab@astro.princeton.edu

(ACVS), which presently contains 50,099 variable stars. The *I* band data is currently being processed and is not yet included in the catalog. ACVS is available both as an online database and a downloadable text file. For details on ASAS equipment and catalogues see Pojmański (1997, 1998, 2000, 2002, 2003), Pojmański and Maciejewski (2004, 2005), Pojmański, Pilecki and Szczygieł (2005). All the ASAS data that is public domain, as well as an online catalogue, are available on the WWW:

<http://www.astro.uw.edu.pl/~gp/asas/asas.html>

<http://archive.princeton.edu/~asas/>

2.2 RR Lyrae Sample in ACVS

ACVS contains a sample of 2212 RR Lyrae stars: 1455 of RRab type and 757 of RRc type. In variable stars with ambiguous classification, we used those for which RR Lyr type is the most probable. Their distribution across the sky in galactic coordinates is shown in Figure 1.

The classification procedure of variable stars in ASAS was based mainly on Fourier parameters of the light curve, JHK colours from 2MASS, and the object's period as described in Pojmański (2002). The full catalogue consists of five parts created between 2002 and 2005, so the classification of the light curves as RR Lyrae stars was based on measurements taken from different time baselines. But we used the longest available baseline (for most objects between HJD 2451800 to HJD 2453800) to refine their periods, which was especially useful for objects from the oldest catalogues. We also used all available data points of reasonable quality (i.e. with flags A and B) in the search for multiperiodic behaviour.

Because the ASAS classification was automatic and allows multiple type assignment we decided to roughly inspect the lightcurves visually to remove variable stars of other types, which were mistaken for RR Lyrae stars. That left us with 1435 RRab and 756 RRc stars. It is important to mention that the inspection was very superficial and excluded only obvious misclassifications among RRab objects, e.g. MIRA type variables. The light curves of RRc type are very similar to EC (i.e. eclipsing contact binary) type, we simply trust the automatic classification, accepting a high rate of misidentification.

The distribution of periods of our RR Lyrae sample is shown in Figure 2. Figure 3 presents two histograms also based on the sample, one of magnitudes in maximum light and the other one of the amplitudes of the light curves.

3 BLAZHKO EFFECT

The shape of the lightcurves of many RR Lyrae stars changes in a nearly periodic fashion, with time-scales of between about five and a thousand or more days; this is called the Blazhko effect (e.g., Smith 1995). Since this shape change is equivalent to periodic phase and amplitude changes of the harmonics which make up the lightcurve, in the frequency domain it is identified through sidebands (additional peaks) in the periodogram near the harmonics of the main pulsation. Physically these peaks may correspond to excited non-radial modes, but the physical nature of the Blazhko effect is still unsettled a century after its discovery. For some

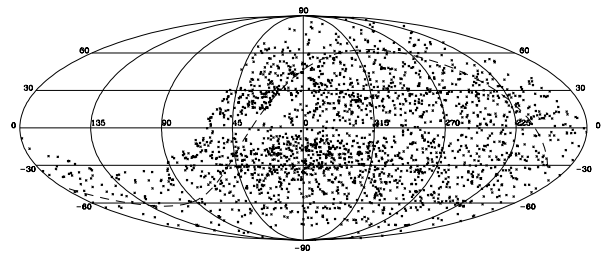


Figure 1. Distribution of RR Lyrae stars from ASAS Catalogue of Variable Stars (ACVS) in galactic coordinates. The dashed line is the equatorial plane.

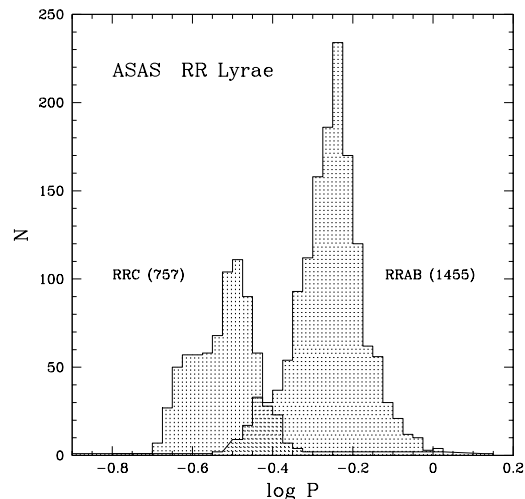


Figure 2. The distribution of periods of the RR Lyrae sample.

stars, which we label BL1, there is a single significant frequency near the main mode. For other stars, which we label BL2, two peaks flank the main frequency with approximately equal frequency spacing (Mizerski 2003, Alcock et al. 2003). There are also some stars with two additional peaks which do not form an equidistant triplet with the main pulsation and others with more than two peaks.

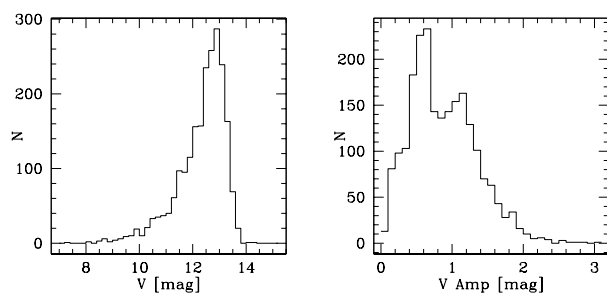


Figure 3. The distribution of *V* magnitudes in maximum light and *V* amplitudes of the RR Lyrae sample.

3.1 Identifying extra frequencies

The method we use for discovering Blazhko stars is a slightly modified version of the method applied by Collinge et al. (2006) to Optical Gravitational Lensing Experiment data. That paper gives a full introduction to the method which we discuss more concisely here.

We first subtract a Fourier series of best-fitting harmonics of the main pulsation period from the data, which is called prewhitening. The number of harmonics to fit was chosen by the method of Kovacs (2005) and depends on an empirical signal to noise level. We next run the CLEAN algorithm (Roberts et al., 1987) on the prewhitened light curves, using 200 iterations and a gain of 0.5, on the frequency band $[0-6 \text{ day}^{-1}]$ with a frequency resolution of $0.125/T$, where T is the overall time baseline of the observations for the given light curve. The peaks are sorted by amplitude, and the noise level is indicated by the 15th largest peak (\mathcal{A}_{15}). By a Monte-Carlo method, we determine how much bigger than that noise level a signal must be to classify as a detection. The Blazhko effect has a period of longer than ~ 5 days, so we define the “Blazhko range” as the frequencies within 0.2 day^{-1} of, but further than $1/T$ from, the main pulsation frequency.

BL1 stars are those with a single peak with amplitude $\mathcal{A} > 2.0\mathcal{A}_{15}$ in the Blazhko range of the CLEANed spectrum. BL2 stars have two frequencies within the Blazhko range, on opposite sides of the main frequency, equidistant to it to within $3.0/T$, and both frequencies must have amplitudes $\mathcal{A} > 1.15\mathcal{A}_{15}$. We follow Alcock et al. (2003) in defining a class of period change (PC) stars that have one or more peaks within $1/T$ of the main frequency with amplitude(s) $\mathcal{A} > 1.3\mathcal{A}_{15}$. The frequency criterion for PC stars means that even if the phenomenon is periodic, we have not yet observed a full cycle; we have only detected a changing lightcurve shape. We note that a long-term amplitude change can also give an extra frequency component near the main frequency, so the PC class is imprecisely named.

During its many iterations, CLEAN produces somewhat biased amplitudes, so after selecting the significant frequencies we refine the fit parameters with a non-linear solver (the Levenberg-Marquardt algorithm; Press et al. 1989); the resulting frequencies and amplitudes are reported in Tables 2, 3, and 4. The best-fitting model is subtracted from the light curve and the amplitude of the highest remaining peak within 0.2 day^{-1} of the main frequency is also reported in Tables 2, 3, and 4. We do not consider this peak significant; it is reported to quantify the level of the noise for completeness studies.

We determined the amplitude thresholds cited above by creating 3 false catalogues, each of them based on the real data sets for each star. In these catalogues the magnitude residuals from the pre-whitening step were randomly swapped among the observation times. We search for peaks in the false catalogues with the CLEAN algorithm and set the amplitude thresholds to allow an acceptable false alarm rate such that about 2% of the stars in each of the categories BL1, BL2, and PC are likely to be spurious.

This method allowed us to determine unambiguous threshold values in the BL2 and PC groups, but it partially failed for the BL1 category. It turned out that false catalogues very often contain a frequency in Blazhko range,

Table 1. Numbers in different categories of RR Lyrae stars exhibiting Blazhko-type behaviour. See section 3.2 for details

	BL1	BL2	BL2x2	PC	Total
RRab	32	41	1	14	1435
RRc	20	29	1	15	756
Total	52	70	2	29	2191

whose amplitude is above the chosen noise level. This is probably a result of high noise in ASAS data. And while the probability to find BL2s in false catalogues is low as it requires two evenly spaced frequencies, it grows rapidly for BL1s, where only one frequency is needed to create a false alarm.

So for BL1s we used a more conservative method of threshold determination. Each prewhitened lightcurve was separated into even-numbered and odd-numbered points in the chronologically ordered data set, making two light curves. Then the search for Blazhko frequency was performed in all three lightcurves—the original and subdivided ones. A frequency must appear at least in two of the three lightcurves to qualify as a true detection. This search was performed for each star in the real and the 3 false catalogues, which allowed us to determine an unambiguous threshold value, because in random realization of the lightcurve such coincidence is less likely to appear.

It turned out that in a real catalog 22 BL1 stars had a Blazhko frequency found in all 3 lightcurve realizations and 30 BL1 stars had it in two, while in false catalogues it never occurred in all 3. Those stars which had a BL1 frequency in all 3 lightcurves are marked with a “*” in the last column of Table 2.

3.2 Objects exhibiting Blazhko effect

The number of unique stars in each of our categories is $(\text{BL1, BL2, PC}) = (52, 70, 29)$; see Table 1 for details.

We see that the number of Blazhko stars, namely 122 objects, is very low; only 5.6% of all RR Lyrae in the Galactic field exhibit any type of a Blazhko effect, which is much lower than the number introduced by Mizerski (2003) for Galactic Bulge (25% RRab and 10% RRC) and Soszynski et al. (2003) for LMC (15% RRab and 6% RRC). The photometric precision of the data is a few percent, which suggests there is serious incompleteness for the Blazhko effect at low amplitudes. Figure 4 (left panel) shows that only a few stars classified as Blazhko have a magnitude $V > 13$, which suggests that detection fails for faint stars, where data scatter is higher.

We also compared our results with previous BL searches in the sky surveys data for our Galaxy. In the recent paper on a similar data quality Northern Sky Variability Survey (Wils, Lloyd and Bernhard 2006) only 34 out of 785 (4.3%) stars exhibit the Blazhko effect, although the time span of the data was just a year. In a Blazhko search in ASAS data done by Wils and Sódor (2005), only 43 objects were identified ($\sim 3\%$), though the search did not include the latest part of ACVS with objects having declinations $\delta > 0$.

The detailed results of our searches are listed in Table 2 for BL1 stars, Table 3 for BL2 and Table 4 for PC objects.

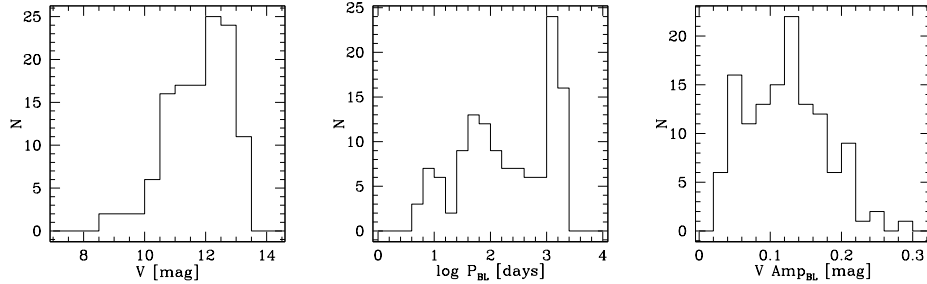


Figure 4. The distribution of V magnitudes of Blazhko stars (left), Blazhko periods (middle) and Blazhko V amplitudes (right) in the RR Lyrae sample.

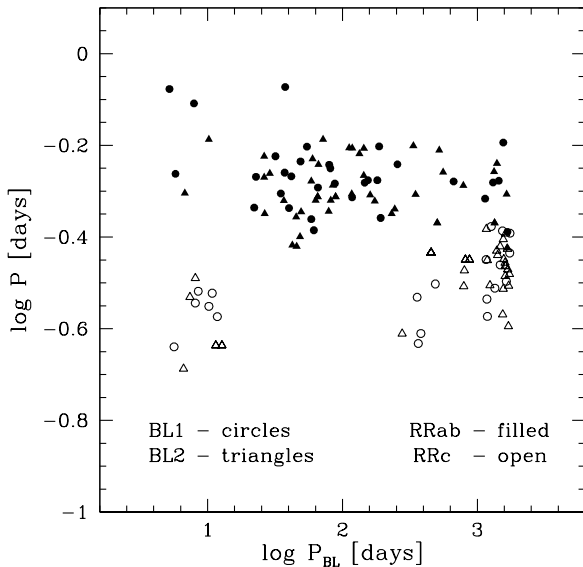


Figure 5. Main pulsation period vs. Blazhko period. The Blazhko periods of RRc stars exhibit a strongly bimodal distribution.

Figure 5 plots the Blazhko period P_{BL} versus main pulsation period P . It is interesting that there is a significant difference in behaviour of RRab (filled symbols) and RRc (open symbols) groups. RRab stars have a relatively uniform distribution in the logarithm of the Blazhko period, whereas RRc stars occupy either the short Blazhko period region around 10 days, or a long P_{BL} area, starting around 300 days with a condensation roughly around 1500 days. That is, we did not observe Blazhko changes with periods above ~ 20 and below ~ 300 days in RRc pulsators. The unusual concentration in very large P_{BL} area, which is often close to the time span of the data, is adding to the peak near $\log(P_{BL}) = 3$ in Figure 4 (middle panel). This may be a false signal due to overall bias and those object might in fact be just exhibiting long period changes (PC). But there are objects having P_{BL} values of 300-500 days, which is 4-5 times shorter than the data span, thus the gap cannot be easily explained as a pile-up of PCs misclassified as BLs.

Jurcsik et al. (2005) found a correlation between the pulsation period and the Blazhko period, such that RR Lyrae with periods $P < 0.4$ d can have P_{BL} of order of days,

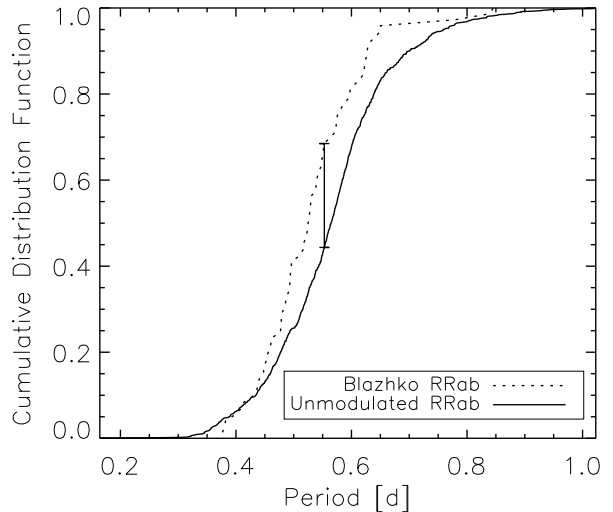


Figure 6. The cumulative distribution function of the main pulsation period for RRab Blazhko stars and those RRab that are not modulated. The maximum difference in the curves is marked with a bar and is highly significant. The lower incidence of the Blazhko effect for stars with long pulsation periods could give fundamental insight to the physical cause of the Blazhko effect, but we suspect that they exist but dropped out of our sample due to misclassification (see text).

while those with longer pulsation periods such as $P > 0.6$ d always exhibit modulation with $P_{BL} > 20$ d. Our Fig. 5 does not support this statement. They also suggested that there is a “continuous transition” between BL1 and BL2 type modulations. While we observe differences in Blazhko behaviour between RRab and RRc groups, which can be due to physical differences in pulsation mechanisms in these groups, we note that BL1 (circles) and BL2 (triangles) occur in roughly constant proportion throughout Fig. 5. This may suggest that both BL1 and BL2 effects have the same origin, it is just that in case of BL1 we do not observe the second equidistant peak present in BL2 category.

Figure 5 also reveals that the number of BL stars falls rapidly for pulsation periods $P > 0.65$ d ($\log(P) > -0.2$). We compared the period distributions for RRab stars exhibiting the Blazhko effect with those that do not. Figure 6 is a plot of the cumulative distribution function of the main pulsation period for Blazhko RRab stars and for RRab

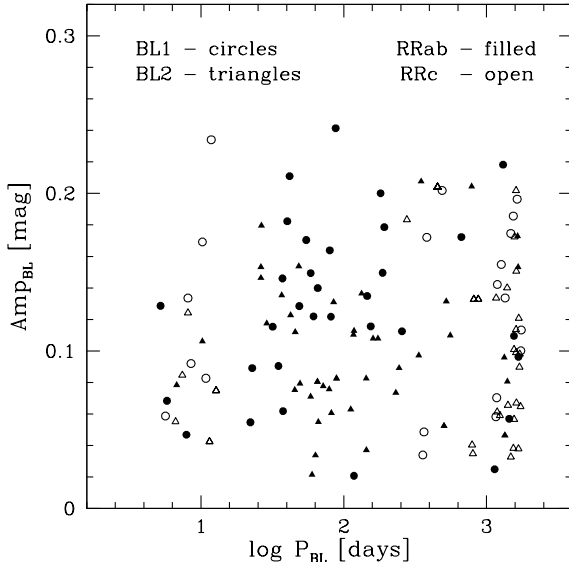


Figure 7. Blazhko amplitude versus Blazhko period.

stars whose lightcurves are not modulated. The maximum difference is 0.241466 which occurs at $P = 0.552945$ d and has a false alarm probability of 4.8×10^{-4} according to the Kolmogorov-Smirnov test, as computed with the KSTWO function from Press et al. (1989). This observation could be important constraint for models of the Blazhko effect, but it may also indicate misclassification of RRab stars that are modulated. That is, lightcurves of BL RRab are not as well-defined as their non-Blazhko counterparts and so have different Fourier parameters, on which the classification of Pojmański (2002) was based. The risk of misclassification is especially strong for long period BL RRab, which may appear as δ Cephei first overtone pulsators if their fourth harmonic is reduced relative to the second harmonic (see Fig. 6 of Pojmański, 2002). If this explanation is true, it would help account for the low percentage of BL stars with respect to other surveys, since there are some Blazhko stars that were not found because we accepted the automatic classification.

We also checked if there is any dependence of Blazhko amplitude on pulsation period. We do not see any significant trend; the distribution seems to be uniform. The right panel in Figure 4 shows the distribution of modulation amplitudes. Similarly, Blazhko amplitude versus modulation period (Fig. 7) does not present any relation. Both long and short Blazhko periods can have an amplitude as small as 0.02 mag and as big as 0.2 mag.

Table 2 contains magnitude, periods and amplitudes for BL1 stars. The main pulsation period is $P = f_0^{-1}$, where f_0 is the main pulsation frequency, and Blazhko period is defined as $P_{BL} = (f_1 - f_0)^{-1}$, where f_1 is the frequency component caused by the Blazhko effect. Thus the negative value of P_{BL} means that the additional frequency is smaller than the main pulsation frequency. This occurs in 10 out of 20 cases of RRc type and only 7 out of 32 of RRab, consistent with previous statistics (eg. Moskalik and Poretti, 2003, Mizerski 2003)

Tables 3 contains magnitude, periods and amplitudes for BL2 stars. The main pulsation period is also $P = f_0^{-1}$, where

f_0 is the main pulsation frequency. Now the Blazhko period is defined as $P_{BL} = (f_{-,+} - f_0)^{-1}$ where $f_{-,+}$ means we choose between Blazhko frequencies (f_- and f_+ , with $f_- < f_0 < f_+$) the one with higher amplitude. The negative value of P_{BL} means that the Blazhko peak of higher amplitude has a frequency lower than the main pulsation. This corresponds to the ratio of $A_-/A_+ > 1$. We see that such case occurs in 13 out of 29 objects of RRc type and 19 out of 41 of RRab.

Finally, Table 4 contains magnitude, period, and amplitude information for PC stars. The designations are the same as in Table 2. For RRab, equal numbers of stars have the modulation frequency lying on left and right side of the main pulsation frequency, which suggests that PC stars may be physically distinct from BL1, and not simply BL1s with periods longer than the dataset.

Three stars (one among RRab and one among RRc groups) have two pairs of equidistant frequencies in the prewhitened spectrum. Their properties are listed in Table 5. Except for SU Col, which we discuss in the next section, these pairs of BL2 peaks are close to one another, probably indicating that the Blazhko effect has an unstable period.

3.3 A star with a rich Blazhko spectrum

In the course of this analysis we identified one star (ASAS 050747-3351.9 = SU Col) that has two clearly distinct pairs of BL2 peaks. In order to look for additional extra frequencies, we first folded the raw light curve and determined, based on the scatter, that a 6 harmonic model would be appropriate. After removing those, we ran the CLEAN (Roberts et al. 1987) algorithm, with a gain of 0.5, for 200 iterations. The frequency grid, of spacing $0.125/T$, ran from 0 day^{-1} to 10 day^{-1} . We then sorted the peaks and identified pairs of peaks which were equidistant across each of the harmonics. Additional frequency components of the Blazhko periods were found surrounding higher harmonics, as well as a candidate for a third Blazhko period. The parameters returned by CLEAN were refined with the Levenberg-Marquardt algorithm according to the model

$$X_m(t) = \mu - \sum_{i=7}^{15} A_i \cos[2\pi f_i(t - T_i)], \quad (1)$$

where the mean magnitude was fit to be $\mu = 12.5980$ and the resulting fits for the other parameters (f_i , A_i , and T_i) are in Table 6.

The identification and removal of these significant frequencies is illustrated in Figure 8. Panel (a) shows a Lomb-Scargle (Lomb 1976, Scargle 1982) periodogram of the raw light curve, with the first four harmonics marked with open triangles. A six harmonic model was fitted by least squares, taking observational errors into account, and subtracted from these data. Panels (b)-(e) show the periodogram of the residual light curves within 0.1 day^{-1} of each of the first three harmonics. Marked with filled triangles are frequencies corresponding to sinusoids that have already been subtracted, whereas marked with open triangles are frequencies identified as significant in the current panel. Panels (b), (c), and (d) correspond to the Blazhko frequencies of $f_{B1} = 0.0112 \text{ day}^{-1}$, $f_{B2} = 0.0152 \text{ day}^{-1}$, and $f_{B3} = 0.0339 \text{ day}^{-1}$, matching Blazhko periods of 89.2 days, 65.6 days, and 29.5 days, respectively. Panels (e) and (f) are

Table 2. Objects exhibiting BL1 effect. A_0 is the amplitude of variation as provided by ACVS and A_1 is the amplitude of Blazhko modulation. See section 3.2 for details.

ASAS ID	V [mag]	P [days]	P_{BL} [days]	A_0 [mag]	A_1 [mag]	A_1/A_0	A_{noise}	Type	Other ID
001141-0144.9	11.757	0.5297456	154.53	0.96900	0.11561	0.11931	0.03080	RRAB	RY Psc
003338-1529.2	11.094	0.5737309	-255.50	0.63800	0.11248	0.17629	0.04258	RRAB	RX Cet *
003706-4317.7	13.288	0.6275343	187.12	1.31000	0.14960	0.11420	0.04399	RRAB	-
011831-6755.1	11.417	0.4057948	1748.86	0.48600	0.11333	0.23319	0.04154	RRC	AM Tuc *
013140-4957.3	12.120	0.4604329	40.17	1.10300	0.18231	0.16529	0.02313	RRAB	NSV00539 *
020752-2651.9	9.482	0.4954335	34.88	1.13400	0.09046	0.07977	0.02382	RRAB	SS For
022637-4119.7	10.078	0.2941932	357.94	0.13300	0.03394	0.25516	0.00517	RRC:	- *
025021-6415.7	12.805	0.5724975	-79.81	1.29000	0.16388	0.12704	0.04324	RRAB/DCEP-FO	RV Hor *
031113-2629.0	11.426	0.5973130	31.81	1.02500	0.11535	0.11253	0.02361	RRAB	RX For
033108+0713.4	10.637	0.5281963	-1442.79	0.17900	0.05694	0.31808	0.01531	RRAB/EC/ESD	-
053022-3234.8	11.772	0.2331114	364.60	0.20100	0.04859	0.24173	0.01282	RRC/EC	-
054230-1622.9	11.853	0.5389135	22.84	0.85900	0.08912	0.10374	0.02721	RRAB	- *
055322-5417.9	12.824	0.2452638	381.58	0.56000	0.17211	0.30735	0.04927	RRC/EC	- *
061401-6128.4	9.307	0.4857445	-117.90	0.46200	0.02076	0.04494	0.00772	RRAB	ST Pic *
062326+0005.8	11.962	0.5501317	37.24	0.62600	0.14603	0.23328	0.03619	RRAB	-
064615-4319.2	13.047	0.3186021	1639.61	0.71200	0.19638	0.27582	0.06734	RRC	-
070854+1919.7	8.691	0.7789192	7.92	0.10300	0.04683	0.45463	0.01725	RRAB	- *
071549-4405.3	13.036	0.3144609	-488.40	0.62600	0.20183	0.32241	0.05343	RRC	-
081933-2358.2	10.452	0.2856671	-8.10	0.28600	0.13358	0.46708	0.06143	RRC/EC	- *
085254-0300.3	12.418	0.2669022	-11.80	0.50900	0.23408	0.45988	0.08576	RRC/EC/ESD	- *
090900-0410.4	10.680	0.3032613	-8.52	0.41400	0.09202	0.22226	0.03856	RRC	- *
093731-1816.2	13.048	0.5209175	87.73	1.23400	0.24140	0.19563	0.05796	RRAB	-
101200+1921.9	10.517	0.4826394	-1141.03	0.85500	0.02489	0.02911	0.12734	RRAB	-
123812-4422.5	12.690	0.5235490	1307.70	1.27800	0.21824	0.17077	0.05501	RRAB:	-
124805-0820.8	11.977	0.5105287	65.69	0.87700	0.13988	0.15950	0.03514	RRAB	-
135740-1202.3	12.180	0.2671226	1189.91	0.44400	0.14218	0.32022	0.03344	RRC	-
135813-4215.1	12.425	0.5231816	-146.01	0.83600	0.13485	0.16131	0.03858	RRAB	-
141025-2244.8	12.496	0.6398808	1556.66	0.82100	0.10950	0.13337	0.03375	RRAB	-
144154-0324.7	11.399	0.2293674	-5.65	0.32000	0.05871	0.18345	0.01463	RRC/EC	- *
145315-1435.9	12.426	0.5400738	41.77	0.93700	0.21095	0.22513	0.05006	RRAB	-
155553-4041.7	11.544	0.5819812	48.82	0.72500	0.12848	0.17721	0.04576	RRAB	NSV07330 *
170223-2422.0	11.340	0.4613693	22.18	0.40300	0.05473	0.13581	0.01484	RRAB	-
172721-5305.9	12.303	0.4354330	58.66	1.25000	0.14944	0.11955	0.02793	RRAB	-
180023-7026.5	12.083	0.3556146	1162.79	0.45700	0.05829	0.12756	0.01622	RRC	-
181215-5206.9	12.589	0.8375462	-5.22	0.67100	0.12865	0.19172	0.01482	RRAB	-
185719-6321.4	12.277	0.4120017	61.39	0.96200	0.12194	0.12675	0.03128	RRAB	-
194502+2434.2	11.723	0.8458661	37.56	0.30200	0.06181	0.20467	0.01263	RRAB/EC/ESD	-
200431-5352.3	10.952	0.3002402	10.82	0.31400	0.08267	0.26329	0.03536	RRC	- *
200556-0830.9	12.753	0.4381966	192.20	1.11600	0.17858	0.16002	0.04252	RRAB	KM Aql
202746-2850.5	11.930	0.4084525	1674.48	0.51900	0.09630	0.18556	0.03482	RRAB/EC/ESD	-
203420-2508.9	11.581	0.5262389	666.44	0.90400	0.17233	0.19063	0.04851	RRAB	-
203749-5735.5	12.248	0.4199162	-1270.33	0.43300	0.15489	0.35771	0.06707	RRC/EC	- *
210741-5844.2	13.219	0.3462376	1479.95	0.68200	0.17462	0.25604	0.05639	RRC/EC	- *
211839+0612.3	11.060	0.2914601	-1176.75	0.48400	0.07032	0.14528	0.01432	RRC	- *
212034+1837.2	11.496	0.5624065	81.30	0.76000	0.12174	0.16019	0.03136	RRAB	-
212331-3025.0	12.288	0.3674420	1739.74	0.47400	0.10016	0.21130	0.02705	RRC/EC	-
213826-3945.0	12.974	0.4107031	-1540.12	0.62300	0.18565	0.29799	0.08610	RRC	- *
221556-2522.6	11.302	0.5467383	5.78	0.77600	0.06836	0.08809	0.01170	RRAB	-
225248-2442.2	12.778	0.5295565	181.20	1.19300	0.20011	0.16774	0.05247	RRAB	-
230659-4354.6	12.660	0.2811062	-10.24	0.39300	0.16923	0.43062	0.04961	RRC/EC/ESD	BO Gru *
231209-1855.4	12.568	0.3079943	-1349.89	0.46800	0.13366	0.28560	0.04982	RRC/EC	- *
232031-1447.9	12.460	0.6269552	54.52	0.58800	0.17040	0.28980	0.04246	RRAB	- *

the periodogram of the final residuals, zoomed in on the first three harmonics and of the entire interval, respectively. The two sets of BL2 frequencies near the main peak—left hand side of panel (b)—is what led us to investigate this star in detail. In some cases apparently significant peaks disappear upon the removal of another peak; this is a symptom of aliasing. An example can be clearly seen when the peak at 4.04 day^{-1} in panel (c) disappears upon removal of the peak at $f_{11} = 2.037 \text{ day}^{-1}$. We used the CLEAN algorithm to avoid precisely this type of confusion.

Despite our efforts using CLEAN, the reality of the third Blazhko period is not conclusively established because there is a peak in the window function at $f' = 2.0027 \text{ day}^{-1}$ which couples f_{B2} to f_{B3} . The following numerical relationships approximately hold:

$$f_{15} - f' \approx f_{12} \quad (2)$$

$$f_{14} + f' \approx f_2 - f_{B2}. \quad (3)$$

Equation 2 implies f_{15} could be a nearly 2 day^{-1} alias of f_{12} . In addition, we note that the fitted parameters of these sinusoids have a large covariance, about half the geometric mean of the individual parameters' variances. Equation 3 gives the reason for this covariance, although our analysis did not identify a significant sinusoid at $f_2 - f_{B2}$; if it exists, it is apparently buried in noise.

The status of SU Col as an RR Lyrae variable was established by Gessner (1985). Berdnikov and Turner (1996) presented an O-C diagram and refined the ephemeris of maximum light, giving:

$$\text{Max HJD} = 2450363.870(2) + 0.48735842(11) \times E. \quad (4)$$

Table 3. Objects exhibiting BL2 effect. A_0 is the amplitude of variation as provided by ACVS and A_- and A_+ are the amplitudes of Blazhko modulation corresponding to the modulation frequency on the left and right side of the main pulsation frequency, respectively. See section 3.2 for details.

ASAS ID	V [mag]	P [days]	P_{BL} [days]	A_0 [mag]	A_- [mag]	A_+ [mag]	A_-/A_+	A_{noise}	Type	Other ID
003514-0415.0	12.758	0.3445751	-1616.29	0.60400	0.14490	0.15073	0.96131	0.02776	RRC/EC	-
012848-1127.2	12.588	0.5166664	-84.99	1.21400	0.13104	0.12332	1.06253	0.01092	RRAB/DCEP-FO	-
020728-5752.2	10.876	0.3750261	1673.36	0.43900	0.04218	0.03796	1.11119	0.00457	RRC	NSV00728
021515-1048.0	10.522	0.6234139	112.05	0.63600	0.09762	0.06289	1.55222	0.01310	RRAB	RV Cet
030534-3116.1	12.525	0.4964538	-6.77	1.47300	0.07832	0.06298	1.24351	0.01973	RRAB	-
031408-3446.4	11.412	0.3124235	-1241.77	0.52400	0.05900	0.04404	1.33957	0.01207	RRC	-
032438-2334.7	12.093	0.6296339	335.29	0.93800	0.12225	0.09725	1.25707	0.00967	RRAB	-
032520-6503.3	11.237	0.4920082	-160.64	0.87700	0.10799	0.10469	1.03147	0.04279	RRAB/DCEP-FO:	X Ret
050747-3351.9	12.048	0.4873552	65.41	1.01100	0.08045	0.10436	0.77090	0.02913	RRAB	SU Col
050747-3351.9	12.048	0.4873552	88.98	1.01100	0.08257	0.08386	0.98464	0.02913	RRAB	SU Col
050838-5602.9	12.098	0.5160761	-786.91	1.08500	0.20443	0.05400	3.78568	0.03188	RRAB	NSV 1856
051508-4137.7	10.447	0.4788368	81.95	0.84300	0.14815	0.06066	2.44245	0.01977	RRAB	RY Col
052402-2247.4	13.400	0.6498517	-10.23	1.19300	0.09961	0.10618	0.93813	0.02691	RRAB	-
052840-5316.2	13.375	0.3678062	-453.43	0.66800	0.20400	0.16895	1.20749	0.05267	RRC	-
053628-3837.0	12.640	0.3714727	-1394.31	0.56600	0.08565	0.14005	0.61157	0.01199	RRC	-
054843-1627.0	12.883	0.3767273	1663.06	0.87900	0.15330	0.16507	0.92875	0.02931	RRAB/RRC:	-
070001-3732.5	11.848	0.4941843	116.96	0.88800	0.13354	0.11041	1.20946	0.02446	RRAB	NSV03331
080249-5913.5	11.747	0.3541891	-1185.26	0.28100	0.05500	0.06132	0.89696	0.01303	RRC/EC/ESD	-
080318-2530.1	10.863	0.2697723	-1542.02	0.42600	0.03821	0.02939	1.29995	0.00559	RRC	NSV03882
085448-8317.0	12.273	0.4778598	-36.79	1.29700	0.13541	0.09648	1.40349	0.03062	RRAB	NSV04350
091349-0919.1	10.707	0.5372290	26.30	0.89800	0.15326	0.15750	0.97310	0.02607	RRAB/DCEP-FO	SZ Hya
094438-4552.6	11.577	0.5735076	66.35	0.94800	0.05499	0.05602	0.98170	0.01491	RRAB	CD Vel
103203-3010.6	11.560	0.3304459	1731.60	0.47500	0.06470	0.06487	0.99744	0.01406	RRC	NSV04885
103246-3423.1	13.391	0.2448541	-277.05	0.77800	0.11921	0.18338	0.65005	0.04180	RRC	-
105303-4954.4	10.758	0.5274139	58.68	0.84800	0.08273	0.07100	1.16520	0.02098	RRAB	AF Vel
110522-2641.0	11.683	0.2944559	-7.40	0.37800	0.08463	0.07400	1.14363	0.02499	RRC	-
112027-4338.8	11.158	0.3795948	1480.38	0.28200	0.03273	0.03557	0.92014	0.02917	RRC/EC/ESD	-
114555-5922.7	11.163	0.4531949	-79.01	1.19400	0.06815	0.07582	0.89891	0.02207	RRAB	BI Cen
120447-2740.7	9.756	0.6503243	71.79	0.61900	0.12521	0.07770	1.61142	0.03368	RRAB	IK Hya
120942-3457.4	13.204	0.3436271	1611.60	0.65900	0.14540	0.09896	1.46928	0.02810	RRC	EL Hya
121206-2612.8	12.652	0.3987747	48.46	1.31500	0.19592	0.15372	1.27450	0.03997	RRAB	-
123030-2602.9	9.806	0.4785475	63.29	0.93500	0.04754	0.03376	1.40824	0.01104	RRAB	SV Hya
132922-0553.0	11.243	0.5763497	1398.99	0.87000	0.14192	0.08057	1.76153	0.03997	RRAB	-
140324-3624.4	10.714	0.4939666	-1650.71	0.97900	0.14793	0.17290	0.85559	0.04442	RRAB	V0674 Cen
141345-2254.7	12.046	0.4479434	26.50	1.00200	0.29592	0.17966	1.64714	0.04185	RRAB	-
150924-4319.6	12.469	0.3821508	42.49	1.14600	0.25505	0.12270	2.07860	0.04271	RRAB	FU Lup
151849-1000.0	12.026	0.3364272	802.95	0.49900	0.16900	0.03488	4.84458	0.08071	RRC	-
153517-2420.2	11.244	0.3067770	1560.06	0.54100	0.06210	0.05660	1.09719	0.01893	RRC	CG Lib
153830-6906.4	12.255	0.6224747	-118.05	0.89300	0.11281	0.08277	1.36289	0.02082	RRAB	-
155552-2148.6	11.379	0.2541338	1699.52	0.45500	0.10083	0.08974	1.12357	0.02034	RRC	-
160204+1728.8	10.718	0.2308114	11.49	0.44100	0.04252	0.05211	0.81599	0.03729	RRC	LS Her
160204+1728.8	10.718	0.2308114	12.76	0.44100	0.07473	0.10049	0.74364	0.03729	RRC	LS Her
162158+0244.5	12.473	0.3238044	-8.11	0.51700	0.12338	0.12424	0.99308	0.02990	RRC/EC	-
162811+0304.3	13.086	0.5970104	-26.28	1.65200	0.13521	0.14638	0.92369	0.03290	RRAB	-
163225-8354.2	8.994	0.5425804	-143.73	0.85300	0.08177	0.08255	0.99053	0.04138	RRAB	UV Oct
172932-5548.3	12.890	0.3273052	-1610.05	0.68200	0.20185	0.16928	1.19245	0.02081	RRC	EZ Ara
174048-3132.6	10.602	0.4272967	-504.03	0.85200	0.05244	0.04493	1.16715	0.01914	RRAB	V0494 Sco
174202-4633.7	10.725	0.3115788	-1706.78	0.49100	0.09802	0.09691	1.01143	0.03052	RRC	-
175911-4926.0	10.108	0.4518593	-49.37	0.93900	0.07659	0.07932	0.96559	0.02219	RRAB	S Ara
183441-6527.0	11.885	0.4769536	-173.70	1.17200	0.10790	0.08878	1.21541	0.02187	RRAB	BH Pav
184758-3744.4	10.255	0.5893445	-59.96	0.59500	0.02151	0.01582	1.35979	0.00532	RRAB	V0413 CrA
192824-1852.4	12.573	0.3563567	1572.33	0.60800	0.17241	0.18557	0.92910	0.05121	RRC	-
193538-7409.9	12.509	0.3499993	1608.49	0.60500	0.11361	0.11671	0.97346	0.02472	RRC/EC	-
195142-6244.1	11.862	0.5514395	557.17	1.13800	0.12042	0.10986	1.09610	0.02272	RRAB	FO Pav
195927-3400.1	11.880	0.3797209	45.69	0.76900	0.14150	0.11196	1.26381	0.03766	RRAB	-
200910-4149.5	12.612	0.4401943	45.39	1.14600	0.08755	0.07533	1.16217	0.02337	RRAB	V2239 Sgr
202044-4107.1	10.931	0.5529452	1331.74	0.86000	0.12189	0.09593	1.27069	0.01562	RRAB	V1645 Sgr
203145-2158.7	11.253	0.3107152	792.83	0.38700	0.04473	0.04035	1.10866	0.00591	RRC/EC	-
204440-2402.7	12.748	0.2053330	-6.64	0.36000	0.05508	0.04355	1.26471	0.01213	RRC/DSCT/EC	-
210129-1513.8	10.466	0.4477465	231.66	1.04200	0.17283	0.07350	2.35140	0.02225	RRAB	RV Cap
212433-5712.1	12.953	0.6051401	-133.38	1.14400	0.13644	0.08877	1.53696	0.02216	RRAB	-
214101+0109.6	12.429	0.6156709	-522.58	0.57200	0.13146	0.09642	1.36346	0.01837	RRAB	-
214719-8739.1	12.338	0.4580005	244.20	1.25100	0.08971	0.08916	1.00624	0.03827	RRAB	RS Oct
215336-8246.8	11.337	0.6218493	144.12	0.98000	0.03715	0.04633	0.80190	0.01014	RRAB	SS Oct
220254-2131.5	10.733	0.3637073	1413.43	0.46100	0.06830	0.06556	1.04181	0.00655	RRC	BV Aqr
222539-0756.5	10.657	0.4052637	1618.65	0.36700	0.07393	0.06703	1.10297	0.01104	RRC	GP Aqr
225131-3006.2	13.101	0.3384769	-1681.80	0.61900	0.11995	0.12080	0.99295	0.02854	RRC/EC	-
225323+0846.1	12.604	0.4930493	-348.58	1.50900	0.18176	0.20762	0.87545	0.04347	RRAB	-
225518-2317.6	12.993	0.3935794	1557.88	0.62100	0.13033	0.10091	1.29156	0.01392	RRC/EC	-
233951-1644.4	12.165	0.3553741	875.96	0.51700	0.16798	0.13284	1.26455	0.05783	RRC	-

Table 4. Objects exhibiting long period changes (PC). See section 3.2 for details.

ASAS ID	V [mag]	P [days]	P_{BL} [days]	A_0 [mag]	A_1 [mag]	A_1/A_0	A_{noise}	Type	Other ID
010117-4556.6	11.700	0.3738269	2085.07	0.27000	0.07760	0.28740	0.02468	RRC	-
011831-6755.1	11.417	0.4057948	-1702.13	0.48600	0.10370	0.21337	0.04154	RRC	AM Tuc
032337+1540.0	9.657	0.2384770	-1738.83	0.13100	0.02283	0.17428	0.00135	RRC/EC/ESD	-
033108+0713.4	10.637	0.5281963	1116.69	0.17900	0.04376	0.24448	0.01531	RRAB/EC/ESD	-
040500-4457.1	12.661	0.5668385	-1533.98	0.77700	0.04583	0.05898	0.01069	RRAB	-
045213-5620.8	13.591	0.3503107	2050.02	0.75400	0.20999	0.27850	0.05707	RRC	-
052406-6925.2	13.183	0.5531259	2668.80	2.21000	0.17673	0.07997	0.01503	RRAB	TY Dor
052840-5316.2	13.375	0.3678062	2178.17	0.66800	0.15844	0.23718	0.05267	RRC	-
062838-3848.5	12.533	0.4834677	2282.06	1.40600	0.10012	0.07121	0.02756	RRAB	-
065307-5935.7	11.474	0.7370705	-2123.14	0.85500	0.05035	0.05889	0.01513	RRAB	IU Car
085816-3022.1	10.603	0.5107257	-2403.27	0.12000	0.02609	0.21744	0.00785	RRAB/DCEP-FO/EC/ESD	-
104749-0308.8	13.043	0.3632554	2236.14	1.01700	0.13533	0.13307	0.05512	RRAB/DCEP-FO/EC	-
112027-4338.8	11.158	0.3795948	-2346.87	0.28200	0.03943	0.13984	0.02917	RRC/EC/ESD	-
112715-2510.4	13.394	0.5768075	-2457.61	1.65600	0.15083	0.09108	0.05732	RRAB/DCEP-FO	-
113701-0600.4	12.573	0.4022837	1880.76	0.60300	0.09181	0.15226	0.01340	RRC/EC	-
140324-3624.4	10.714	0.4939666	-1650.71	0.97900	0.17290	0.17661	0.04442	RRAB	V0674 Cen
151849-1000.0	12.026	0.3364272	-2192.98	0.49900	0.03489	0.06991	0.08071	RRC	-
151951-0950.0	13.376	0.3235636	-8591.07	0.70000	0.00310	0.00442	0.02170	RRC:	-
154504+1736.7	12.825	0.5736250	1309.24	1.27500	0.09460	0.07420	0.06932	RRAB	-
161301-2406.9	12.412	0.6024391	2036.66	0.42700	0.07116	0.16665	0.01786	RRAB:	-
195927-3400.1	11.880	0.3797209	-2285.19	0.76900	0.12301	0.15996	0.03766	RRAB	-
210741-5844.2	13.219	0.3462376	-1839.25	0.68200	0.16950	0.24853	0.05639	RRC/EC	-
212045-5649.2	12.383	0.3680388	2286.76	0.26300	0.05229	0.19882	0.01971	RRC/EC	-
212756-6702.6	12.726	0.3449728	2410.80	0.42700	0.08608	0.20159	0.02752	RRC	-
220454-6635.0	12.051	0.5640177	1722.65	0.88100	0.13549	0.15379	0.05189	RRAB	NSV14009
221039-5049.8	12.322	0.3306480	-1720.28	0.69900	0.15014	0.21479	0.05082	RRC	-
224131-0628.6	11.859	0.5744469	-1771.17	0.72700	0.15084	0.20748	0.02283	RRAB	HH Aqr
225559-2709.9	12.709	0.3103066	-2197.80	0.37300	0.08234	0.22075	0.01736	RRC/EC	-
232342-4157.4	12.716	0.4424689	-2144.08	0.32600	0.06987	0.21434	0.00811	RRC/EC/ESD	-

Table 5. RR Lyrae Blazhko stars with two pairs of BL2s. See section 3.2 for details.

ASAS ID	V [mag]	A_0 [mag]	P [days]	P_{BL} [days]	A_1 [mag]	A_2 [mag]	A_-/A_+	Type	Other ID
050747-3351.9	12.048	1.01100	0.4873552	65.8 89.3	0.08045 0.08257	0.10436 0.08386	0.77090 0.98464	RRAB	SU Col
160204+1728.8	10.718	0.44100	0.2308114	11.5 12.8	0.04252 0.07473	0.05211 0.10049	0.81599 0.74364	RRC	LS Her

The uncertainties are in parentheses, indicating the precision of the final and final two digits for epoch and period, respectively.

The maximum with number $E = 5008$ is near the center of our dataset, and gives a time of maximum $C = 2452804.561$. Although the cadence of our dataset does not allow individual maxima to be found, the nearby maximum of the six harmonic model is at $O = 2452804.558 \pm 0.010$, matching the published ephemeris to within the error ($O - C = 0.002 \pm 0.010$). Our best-fitting main period of $0.487355 \text{ d} \pm 2 \times 10^{-6} \text{ d}$, also marginally fits the ephemeris of equation 4.

The Hipparcos and Tycho Catalog (Perryman and ESA 1997) reported SU Col as an RR Lyrae as well, reporting the epoch of maximum as $O_H = 2448500.2120 \pm 0.0010$. The uncertainty was only reported to order-of-magnitude, and is based on a three harmonic model; judging by the folded light curve it is probably at least a factor of a few too low. This corresponds to maximum number $E = -3825$, whose calculated value is $C_H = 2448500.2114$, giving $O - C = 0.0006 \pm 0.0022$. Therefore equation 4 satisfies three modern data sets over a span of about fifteen years, despite the complication that the Blazhko effect causes on the time of maximum light.

The status of SU Col as a Blazhko star has not been previously recognized. Wils, P. and Sódor (2005) analyzed the ASAS RR Lyrae stars for Blazhko behavior, although we suspect that SU Col was not analyzed because its folded light curve looks like it is affected by noise rather than the Blazhko effect, and visually inspecting the folded light curves was their first cut. Kovacs (2005) also identified Blazhko stars in ASAS, however, he restricted his attention to stars whose metallicity was already measured.

Future observations with a high cadence, spanning a few hundred days, would be extremely valuable for understanding the multiply periodic nature of the Blazhko effect in this star, although a campaign with telescopes distributed in longitude may be necessary to resolve all aliases. Such a campaign has recently reported the similar double Blazhko behavior for UZ UMa (Sódor et al. 2006). SU Col is considerably brighter than the class of objects with two sets of BL2 peaks found by Collinge et al. (2006), so even time-resolved spectroscopy is not prohibitive. Discovering rare objects that are bright enough to follow up is one of the strengths of wide-field surveys like ASAS, and we urge follow-up observations of this object.

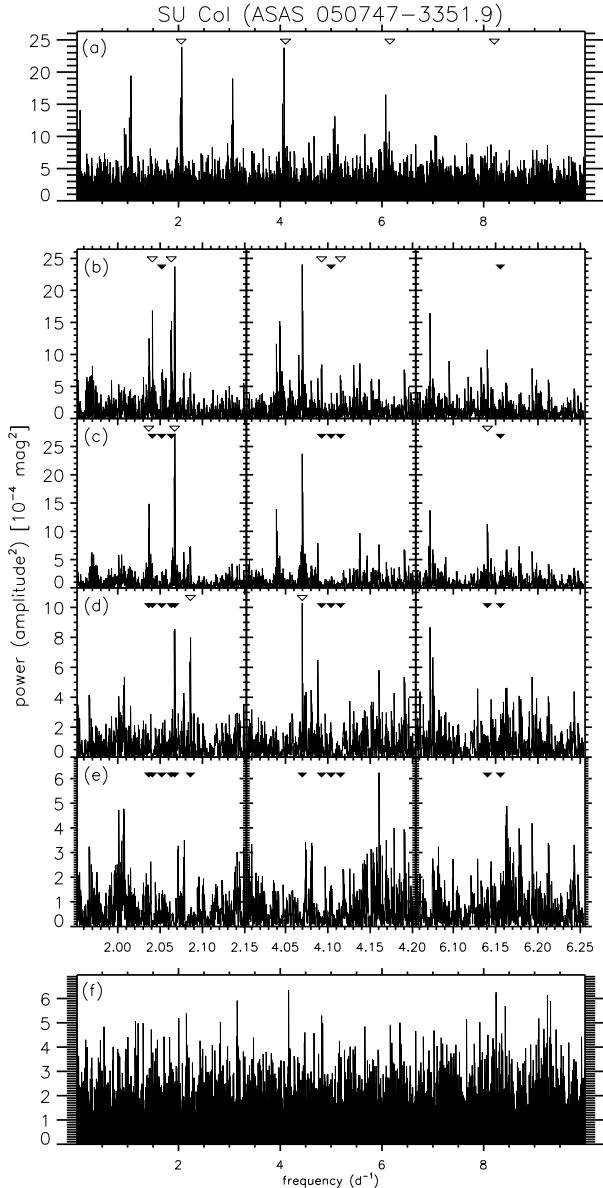


Figure 8. An iterative subtraction of extra frequency components of SU Col illustrates the rich multiperiodic behaviour of this Blazhko star. (a) The Lomb-Scargle periodogram of the raw light curve. (b) Periodogram after removing frequency sinusoids at the main frequency and 5 higher harmonics. The three panels are zoomed in on the region surrounding the first three harmonics. A number of Blazhko peaks are noticeable. (c, d, e) Periodograms after removing the extra peaks associated with f_{B1} , f_{B2} , and f_{B3} respectively (see table 7). (f) The final periodogram after subtracting the 15 peaks listed in Table 6. In each panel, open triangles identify the peaks that are most significant, and filled triangles identify frequencies at which peaks have already been subtracted. See section 3.3.

4 DOUBLE-MODE RR LYRAE

RRd variables are objects pulsating in two radial modes: the fundamental mode and the first overtone. Characteristic is the period ratio of these modes, $P_1/P_0 \approx 0.744$, where P_0 and P_1 correspond to the periods of fundamental mode and the first overtone respectively. So far, 24 such isolated

Table 6. Best-fitted parameters for the detected frequencies in the Blazhko star SU Col. The parameters listed below refer to equation 1. Times of light maximum are listed as HJD-2450000. See section 3.3.

f (day $^{-1}$)	A (mag)	T (day)	note
2.0518901	0.3431	2804.6078	f_1
4.1037803	0.1517	2804.5774	$f_2 = 2f_1$
6.1556702	0.0980	2804.5569	$f_3 = 3f_1$
8.2075605	0.0558	2804.5484	$f_4 = 4f_1$
10.259451	0.0384	2804.6462	$f_5 = 5f_1$
12.311340	0.0255	2804.6246	$f_6 = 6f_1$
2.0407786	0.03823	2804.6775	$f_7 = f_1 - f_{B1}$
2.0631858	0.04373	2804.4963	$f_8 = f_1 + f_{B1}$
4.0926081	0.02802	2804.6302	$f_9 = f_2 - f_{B1}$
4.1149220	0.02840	2804.5249	$f_{10} = f_2 + f_{B1}$
2.0366963	0.04252	2804.5442	$f_{11} = f_1 - f_{B2}$
2.0671779	0.04370	2804.5708	$f_{12} = f_1 + f_{B2}$
6.1403548	0.02972	2804.5370	$f_{13} = f_3 - f_{B2}$
2.0857132	0.02649	2804.6723	$f_{14} = f_1 + f_{B3}$
4.0697479	0.03106	2804.5647	$f_{15} = f_2 - f_{B3}$

objects have been detected in the field of our Galaxy, 17 of them is listed by Wils (2006, see references therein) and 7 by Bernhard & Wils (2006), without including fainter objects of the Galactic Bulge (Mizerski, 2003; Moskalik & Poretti, 2003; Pigulski et al., 2003), and the foreground stars of the dwarf galaxy in Sagittarius (Cseresnjcs, 2001); 13 of them were found in the ASAS data.

Very useful in the study of RRd stars is a Petersen diagram (Petersen 1973), on which the fundamental mode period (P_0) is plotted against the ratio of the overtone and fundamental mode periods (P_1/P_0). Several attempts were made to constrain theoretically the region occupied by RRd stars on a Petersen diagram (Bono et al. 1996, Popielski et al. 2000, Bragaglia et al. 2001, Kovacs 2001). Most recently Szabo et al. (2004) combined both the double mode pulsational and evolutionary theories to construct such a theoretically permitted region. We searched a slightly bigger region ($0.40 \leq P_0 \leq 0.65$ and $0.735 \leq P_1/P_0 \leq 0.755$) for RRd variables without putting any additional constraints. The condition that a star had to fulfill to classify as a RRd candidate was that the ratio of the two highest amplitude frequencies falls within the desired period ratio range. This procedure provided us with 35 candidates.

We visually examined those and 16 turned out to be spurious detections. So in our search for multiperiodicity in ASAS data we detect 19 double mode RR Lyrae variables, among which 4 are newly identified RRd stars. This sums up to 17 RRd stars altogether discovered in ACVS, out of 28 objects now known in the field of our Galaxy (on both southern and northern hemisphere), giving the ASAS project the majority of discoveries. The lightcurves of newly discovered objects, phased with both pulsation periods are given in Figure 9.

Surprisingly, we did not detect 4 objects that were discovered as RRd before and should be present in the ASAS database. After a closer investigation of these objects we found that two of them, namely ASAS 030528-3058.7 (Bernhard and Wils, 2006) and CU Com = ASAS 122447+2224.5 (Clementini et al., 2000) are phased in ACVS with one of the aliases of the true period, so the period ratio fell outside

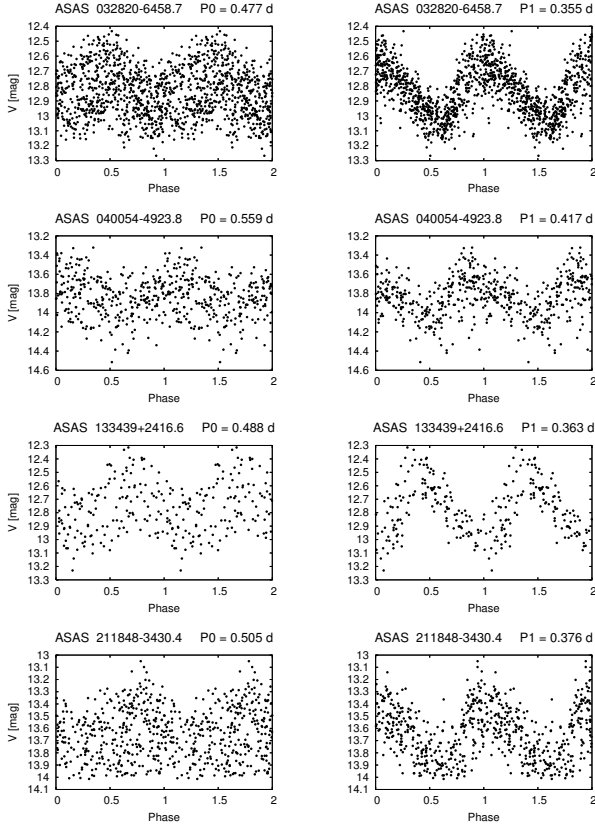


Figure 9. Four newly discovered double-mode pulsators are represented in 4 rows. Each row contains a lightcurve phased with the main pulsation period (left) and the first overtone period (right). See section 4 for details.

the searched region. For the third one (Jerzykiewicz and Wenzel, 1977), namely AQ Leo = ASAS 112355+1019.0, we did not find a significant peak among 50 highest that would correspond to the second pulsation period. However, the lightcurve phased with this period has a modulation that appears significant, which apparently suggests that the CLEAN algorithm failed in this case. The fourth case was an object found by Wils et al. (2006) in NSVS data in an overlap region, namely V458 Her = ASAS 170831+1831.3. We do not confirm any significant secondary frequency in this light curve with the longer dataset.

The incidence ratio, which we define as a number of double mode pulsators divided by the number of RRc stars is $RRd/RRc = 0.025$. This value is small, comparing to the one determined by Alcock et al. (2000) for the LMC, which is 0.134. The ratio for the Galactic bulge calculated by Mizerski (2003) is 0.007.

Parameters of these objects, such as their coordinates, magnitudes, pulsation periods and amplitudes, are listed in Table 7. Also another star ID is given if applicable and a reference to the discovery paper. For stars that are new discoveries, there is a “*” instead of a reference. One of the newly found double mode stars, namely 032820-6458.7 (or SW Ret), is a secure detection based on its period ratio of 0.744417, but it is classified in GCVS as W UMA type

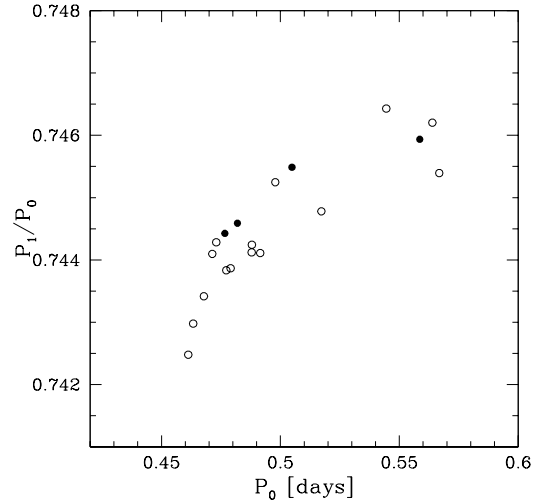


Figure 10. A Petersen diagram for galactic field RRd variables discover during multiperiodicity search on ASAS data. Known objects are plotted with open circles, while newly identified stars are drawn with filled circles. See section 4 for details.

eclipsing variable. However, due to slope asymmetry, ACVS unambiguously classifies this object as an RRc star.

It is known that the majority of RRd stars have a first pulsation mode with a lower amplitude than the first overtone (eg. Alcock et al. 2000). The ASAS detections confirm this: 18 out of 19 objects have amplitude ratio $A_1/A_0 > 1$.

Figure 10 shows a Petersen diagram for double-mode RR Lyrae in ASAS data. All stars follow the sequence observed up to date by many RR Lyrae (see Fig. 13 in Clementini et al. 2004). The new discoveries on our diagram are plotted with solid circles and known objects with open circles.

5 SUMMARY

We performed a multiperiodicity search in the ASAS Galactic field RR Lyrae data, consisting of 1435 R Rab and 756 RRc stars. It resulted in finding 160 objects, 122 of them exhibiting Blazhko effect (BL), 29 long period changes (PC), and 19 double-mode behaviour (RRd stars).

There are 73 BL stars inside the R Rab group, and 49 in RRc, giving a total of 5.6% BL in the whole sample, which is few times less than the percentage observed in Magellanic Clouds and Galactic Bulge, but similar to the number found in previous searches in Galactic field survey catalogs. The analysis of the Blazhko sample reveals a significant difference between the behaviour of R Rab and RRc groups. While R Rab stars have a wide, unimodal distribution in the Blazhko period, RRc stars occupy either the short Blazhko period region around 10 days, or a long P_{BL} area, starting around 300 days, with a condensation roughly around 1500 days. There is a lack of Blazhko stars among high period ($P > 0.65$ d) R Rab stars, which may give insight into the physics of the Blazhko effect, but we suspect simply indicates the misclassification of R Rab stars. We do not confirm any correlation between the pulsation period and the Blazhko

Table 7. Parameters for double-mode RR Lyrae stars (RRd) found in ASAS data. See section 4.

ASAS ID (RA DEC)	V [mag]	P_0 [days]	A_0 [mag]	P_1 [days]	A_1 [mag]	P_1/P_0	A_1/A_0	Other ID	Reference
032820-6458.7	12.565	0.4766242	0.06576	0.3548111	0.17981	0.7444253	2.73445	SW Ret	*
040054-4923.8	13.322	0.5585883	0.10210	0.4166705	0.16466	0.7459348	1.61275	-	*
081610-6644.8	12.362	0.5172180	0.14206	0.3852143	0.20912	0.7447813	1.47211	GSC 8936-2145	(Wils & Otero 2005)
084747-0339.1	10.530	0.5639063	0.07625	0.4207890	0.19765	0.7462037	2.59222	GSC 4868-0831	(Wils & Otero 2005)
122509-2139.9	12.186	0.5445154	0.03287	0.4064419	0.19761	0.7464286	6.01242	-	(Bernhard & Wils 2006)
133439+2416.6	12.440	0.4879017	0.12370	0.3630583	0.22837	0.7441218	1.84618	BS Com	(Bragaglia et al. 2003)
141539+0010.1	13.353	0.4819318	0.11592	0.3588418	0.18171	0.7445904	1.56757	-	*
151735-0105.3	10.965	0.4713494	0.14849	0.3507304	0.21001	0.7440985	1.41430	V0372 Ser	(Garcia-Melendo et al. 2001)
173726+1122.4	12.755	0.4633236	0.16939	0.3442391	0.17301	0.7429777	1.02134	V2493 Oph	(Garcia-Melendo & Clement 1997)
183952-3200.9	11.814	0.4612583	0.20017	0.3424752	0.17871	0.7424802	0.89283	GSC 7411-1269	(Wils & Otero 2005)
184035-5350.7	12.211	0.4790651	0.06790	0.3563601	0.10085	0.7438656	1.48532	-	(Bernhard & Wils 2006)
193933-6528.9	12.887	0.4915148	0.16877	0.3657414	0.20259	0.7441106	1.20034	GSC 9092-1397	(Wils 2006)
195612-5043.7	12.120	0.4678191	0.13216	0.3477846	0.15472	0.7434169	1.17070	GSC 8403-0647	(Wils & Otero 2005)
210726+0110.3	13.062	0.4772373	0.16996	0.3549859	0.21570	0.7438352	1.26906	-	(Bernhard & Wils 2006)
211848-3430.4	12.841	0.5048597	0.10230	0.3763662	0.21639	0.7454867	2.11516	-	*
212721-1908.0	13.064	0.4730220	0.13103	0.3520623	0.19165	0.7442830	1.46258	NSV13710	(Bernhard & Wils 2006)
213437-4907.5	11.997	0.4879954	0.14027	0.3631872	0.19332	0.7442432	1.37818	Z Gru	(Wils 2006)
230449-3345.3	12.995	0.4978410	0.14390	0.3710152	0.21172	0.7452483	1.47130	-	(Bernhard & Wils 2006)
235622-5329.4	12.576	0.5668088	0.09557	0.4224954	0.19555	0.7453932	2.04624	NSV14764	(Bernhard & Wils 2006)

period. Also no visible differences between BL1 and BL2 groups suggest that the same mechanism is responsible for the Blazhko effect in both cases.

During our study we discovered the Blazhko effect with multiple periods (BL2x2) in object ASAS 050747-3351.9 = SU Col. were identified with periodogram peaks near the first three harmonics of the main pulsation.

We also identified 19 double-mode RR Lyrae, 4 of them being new discoveries, one of these (SW Ret) being reclassified from an eclipsing contact binary to a RR Lyrae variable.

ACKNOWLEDGMENTS

We would like to thank G. Pojmański and B. Paczyński for being great advisors. We also thank T. Mizerski for helpful discussions. This research has made use of the SIMBAD database, operated at CDS, Strasbourg, France. This work was supported by the MNiSW grant N203 007 31/1328.

REFERENCES

Alcock, C., et al., 2000, *ApJ*, 542, 257
 Alcock, C., et al., 2003, *ApJ*, 598, 597
 Bailey, S.I., Pickering, E.C., 1902, *Ann. Astron. Obs. Harvard Coll.*, 38, 1
 Berdnikov, L.N. and Turner, D.G., 1996, *IBVS*, 4389, 1
 Bernhard, K., Wils, P., 2006, *IBVS* 5698
 Bono, G., Incerpi, R., Marconi, M. 1996, *ApJ*, 467, 97
 Bragaglia et al., 2003, in: *Annual Report, Osservatorio Astronomico di Bologna*
 Clementini G., di Tomaso S., di Fabrizio L., Bragaglia A., Merighi R., Tosi M., Caretta E., Gratton R.G., Ivans I.I., Kinard A., Marconi M., Smith H.A., Wilhelm R., Woodruff T., Sneden C., 2000, *AJ*, 120, 2054
 Clementini, G., Corwin, T.M., Carney, B.W., Sumerel, A.N. 2004, *AJ*, 127, 938
 Collinge, M., Sumi, T., and Fabrycky, D., 2006, *ApJ*, 651, 197
 Cseresnjcs P., 2001, *A&A*, 375, 909
 Duffau, S., Zinn, R., Vivas, A. K., Carraro, G., Mendez, R. A., Winnick, R., Gallart, C., 2006, *ApJ*, 636, 97
 Eddington, A.S. 1917, *Obs*, 40, 290
 Garcia-Melendo E., Clement M., 1997, *AJ*, 114, 1190

Garcia-Melendo E., Henden A.A., Gomez-Forrellad J.M., 2001, *IBVS*, 5167
 Gessner, H. 1985, *MitVS*, 10, 155
 Jerzykiewicz M., Wenzel W., 1977, *AcA*, 27, 35
 Jurcsik, J., Szeidl, B., Nagy, A., Sódor, Á., 2005, *AcA*, 55, 303
 Kovacs, G. 2001, *A&A*, 375, 469
 Kovacs, G. 2005, *A&A*, 438, 227
 Lomb, N.R., 1976, *Ap&SS*, 39, 447
 Mizerski, T., 2003, *AcA*, 53, 307
 Moskalik P., Poretti E., 2003, *A&A*, 398, 213
 Perryman, M.A.C., and ESA 1997, *The HIPPARCOS and TYCHO catalogues* (Noordwijk, Netherlands; ESA Publishing Division)
 Petersen, J. O., 1973, *A&A*, 27, 89
 Pigulski A., Kolaczowski Z., Kopacki G., 2003, *Acta Astron.*, 53, 27
 Pojmański, G. 1997, *AcA*, 47, 467
 Pojmański, G. 1998, *AcA*, 48, 35
 Pojmański, G. 2000, *AcA*, 50, 177
 Pojmański, G. 2002, *AcA*, 52, 397
 Pojmański, G. 2003, *AcA*, 53, 341
 Pojmański, G., and Maciejewski, G. 2004, *AcA*, 54, 153
 Pojmański, G., and Maciejewski, G. 2005, *AcA*, 55, 97
 Pojmański, G., Pilecki, B., Szczygiel, D. 2005, *AcA*, 55, 275
 Popielski, B.L., Dziembowski, W.A., Cassisi, S. 2000, *AcA*, 50, 491
 Press, W.H., Teukolsky, S.A., Vetterling, W.T., & Flannery, B.P. 1989, *Numerical Recipes in C* (2d ed.; Cambridge; Cambridge University Press)
 Roberts, D.H., Lehar, J., & Dreher, J.W., 1987, *AJ*, 93, 968
 Scargle, J.D., 1982, *ApJ*, 263, 835
 Shapley, H. 1914, *ApJ*, 40, 448
 Shapley, H. 1918, *ApJ*, 48, 89
 Smith, H.A., 1995, *RR Lyrae Stars* (Cambridge, UK: Cambridge University Press)
 Sódor, Á., Vida, K., Jurcsik, J., Váradi, M., Szeidl, B., Hurta, Zs., Dékány, I., Posztobányi, K., Vityi, N., Szing, A., Kuti, A., Lakatos, J., Nagy, I., Dobos, V., 2006, *IBVS*, 5705
 Soszynski, I., Udalski, A., Szymanski, M., Kubiak, M., Pietrzynski, G., Wozniak, P., Zebrun, K., Szewczyk, O., Wyrzykowski, L., 2003, *Acta Astron.*, 53, 93
 Szabó, R., Kollth, Z., Buchler, J. R., 2004, *A&A*, 425, 627
 Wils, P., 2006, *IBVS*, 5685
 Wils, P., Lloyd, C., Bernhard, K. 2006, *MNRAS*, 368, 1757
 Wils, P., Otero, S.A., 2005, *IBVS*, 5593, 1
 Wils, P. and Sódor, Á., 2005, *IBVS*, 5655, 1